Supplementary Material

Cr(III)-bearing schwertmannite transformation by Fe(II)-oxalic acid catalyzed: complexation of Fe(III)/oxalate and nanoscale redistribution of Cr/C

Qian Yao [a, b], Limiao Cai [a, b], Xiaofei Li [a, b], Xiaohu Jin [a, b], Guining Lu [a, b], Chuling Guo [a, b], Weilin Huang [c], Zhi Dang [a, b], Xiaoyun Yi [a, b, *]

[a] School of Environment and Energy, South China University of Technology, Guangzhou 510006, People's Republic of China

[b] The Key Lab of Pollution Control and Ecosystem Restoration in Industry Clusters, Ministry of Education, School of Environment and Energy, South China University of Technology, Guangzhou 510006, People's Republic of China

[c] Department of Environmental Sciences, Rutgers University, New Brunswick, NJ, 08901, USA

[*]Corresponding authors: School of Environment and Energy, South China University of Technology, Guangzhou 510006, People's Republic of China; Tel: +86-20-39380508, Fax: +86-20-39380508

E-mail addresses: xyyi@scut.edu.cn

13 Pages
7 Sections
1 Table
11 Figures

Section S1. Chemicals, materials

Ferrous sulfate heptahydrate ($FeSO_4 \cdot 7H_2O$), sodium hydroxide (NaOH), hydrochloric acid (HCl), hydrogen peroxide (H_2O_2), Sodium chloride (NaCl), Ferrous chloride tetrahydrate ($FeCl_2 \cdot 4H_2O$) and ammonium acetate (CH_3COONH_4) were obtained from Aladdin reagent company, Shanghai. Oxalic acid dihydrate ($H_2C_2O_4 \cdot 2H_2O$, Shanghai Macklin Biochemical Co., Ltd) was used as C source. All solutions in all experiments were prepared with deionized water that produced by a Millipore system (≥ 18 MΩ cm). All glassware was repeatedly cleaned by soaking in 1 M HCl for 12 h and thoroughly rinsed.

Section S2. Synthesis of Schwertmannite

In brief, 100 g $FeSO_4 \cdot 7H_2O$ was dissolved into 10 L distilled water at 25 °C, and then 50 mL H_2O_2 (32%) was added. The solution gradually becomes dark-red material precipitation. After incubating for 24 h, the ochre-colored precipitates were washed by the sulfuric acid solution (pH $\approx$ 2.5) and distilled water repeatedly until the specific conductance was less than 20 μs cm^{-1}. The remaining precipitates were finally dried at 40 °C and pulverized to pass through a 200-mesh sieve before use. Cr(III)-substituted schwertmannite (Cr-Sch) was achieved by following the same procedure as described above, except for the addition of 13.1g Cr(VI) prior to the H_2O_2.[1]

Section S3. Cr-Sch aging and transformation experiments

The transformation experiments were conducted in PTFE bottles covered by the

aluminum foil to avoid photochemical interferences at room temperature (25 °C). The deoxygenated solutions and dried minerals were maintained for 24 h inside the anaerobic chamber to remove residual O_2 via a Pd catalyst. The transformation of Cr-Sch was initiated by adjusting and maintaining suspension pH to 3.5/4.5/5.5/6.0/6.5/7.0, respectively. Briefly, 500 mg of synthetic Cr-Sch was added to sufficient solution inside a 500-mL anaerobic bottle (1.0 g/L). The pH of the reaction solution was maintained at 3.5/4.5/5.5/6.0/6.5/7.0 using 10 mM NaOH with 10 mM NaCl as the background electrolyte. Stock solutions of oxalic acid and Fe(II) were prepared by dissolving oxalic acid and $FeCl_2 \cdot 4H_2O$ in a background solution before use. Appropriate quantities of oxalic acid stock solutions were added to the different pH schwertmannite suspensions, resulting in oxalic acid loadings of 0, 1 mM. The transformation experiments were initiated by adding the requisite volume of freshly prepared $FeCl_2$ stock solution to the reaction vessel to achieve a 1-mM Fe(II) concentration. A set of experiments with adding 1 mM Fe(II) and with different concentration oxalic acid was also conducted to investigate the impact of oxalic acid on the transformation of schwertmannite under anaerobic conditions. The selected pH and Fe(II) concentration were associated with the schwertmannite-rich environment.[2,3] The 10 mM NaOH and HCl were used for pH control throughout the experiment. At 0, 1, 2, 4, 8, 24, 48, 96, and 192 h, subsamples from each treatment were sacrificed. The aqueous phase was filtered through a 0.22 μm polyethersulfone membrane, and the filtrate was immediately acidified to pH <2 with HCl. The remaining suspension was centrifuged and washed three times with deoxygenated deionized water, and the

residual solid phase was freeze-dried for further solid phase analysis. The triplicate experiments were carried for determining the repeatable and accuracy.

Section S4. In situ ATR-FTIR experiments

In situ attenuated total reflectance-fourier transform infrared spectrometry (ATR-FTIR) experiments were conducted to using a Thermo-Nicolet iS10 FTIR spectrometer instrument equipped with a liquid-nitrogen cooled mercury cadmium telluride (MCT) detector. In situ ATR-FTIR spectra were recorded on a FTIR spectro-photometer equipped with a multi-bounce horizontal ATR accessory and flow cell. A thin film of immobilized Sch particles (~4 mg) was coated on the surface of the horizontal ZnSe crystal by drying Sch suspension overnight in the glove box. The Sch layer was allowed to softly flush out the loosely adhere particles and impurities with the ultrapure water, followed by a preliminary equilibration with 10 mM NaCl solution (pH 3.0) after which a spectrum was collected as a background. And then 0.1 mM oxalic acid solution (pH 3.5/4.5/5.5/6.0/6.5/7.0) flowed over Sch layer through a peristaltic pump at a rate of 0.5 mL/min. In addition, Fe(II)/oxalic acid ratio (1:1) was also carried. All of the spectra were collected at 25 °C in the range of 400-4000 cm^{-1}, with a resolution of 4 cm^{-1} and 128 scans. At the end of each batch experiments, no corrosion of the Sch film was observed.

Section S5. The Peakfit software and 2D-COS Analysis

After smooth and baseline correction for the IR spectra using Omnic 8.2 software, two-dimensional correlation spectroscopy (2D-COS) analysis was

performed using 2D-shige software (Shigeaki Morita, Japan). The sequential order of intensity change between bands ν1 and ν2 can be obtained from the sign of the synchronous correlation peak Φ (ν1, ν2) and asynchronous correlation peak Ψ (ν1, ν2) under well-established principles.[4, 5] Briefly, the change in the spectral intensity at band ν1 occurs prior to that at ν2 if Φ (ν1, ν2) and Ψ (ν1, ν2) have the same signs; while the order is reversed if Φ (ν1, ν2) and Ψ (ν1, ν2) have opposite signs. The changes at ν1 and ν2 occur simultaneously if Ψ (ν1, ν2) is zero.

For a better identification of peaks, the peak fittings of all IR spectra were carried out with Peakfit v.4.12 software. The spectra were baseline corrected using the Omnic baseline correction algorithm. Because the second derivative presents a much sharper band and better resolution than the original, the second derivative IR spectra were employed in the peak fitting. The Savitsky-Golay second derivatives were calculated to assist band identification using an order of 4 and with the number of points depending on the signal-to-noise ratio in the original spectra. The goodness of fit R factor in all of the fitted spectra was greater than 0.999.

Section S6. Characterization of transformed solid products

The solid samples were analyzed through X-ray diffraction (XRD, D8 Advance, Bruker) using Cu Kα radiation (λ = 1.5418 Å, 40 kV, and 40 mA). Diffractograms were recorded in the 2θ range of 10° to 80° with a step size of 0.013°. The surface morphology and particle size of the solid samples were characterized using scanning electron microscopy (SEM, Carl Zeiss Microscopy, Germany). The Mössbauer

measurements were conducted at 13 K through a conventional spectrometer (Germany, Wissel MS-500) using A 57 Co(Rh) source with an activity of 25 mCi in the transmission geometry with the constant acceleration mode. The obtained spectra were fitted using the Recoil software via Voigt-based fitting (VBF) analysis.[6]

Section S7. Spherical aberration corrected scanning transmission electron microscopy (Cs-STEM) analysis experiments

Solid sample (~0.1 mg) was dispersed ultrapure acetone in 2 ml cover centrifuge tube and then ultrasonicated for 30 min. To prevent Fe oxide transformation during ultrasonication, the vessel with the suspension and acetone was sonicated in cold water. A 10 μL aliquot of sonicated suspension was pipetted onto a 5 nm thick Si_3N_4 TEM membrane (SiMPore Inc., USA) that was used to prevent the interference of the C element back-ground. Samples were dried for 60 min in the glove box. The prepared samples were analyzed in an analytical transmission electron microscope (TEM) (Titan Themis 200, FEI, USA) with a field emission gun and a probe Cs corrector (CEOS GmbH). Mineral morphology was observed through high angle annular dark field (HAADF) and bright field (BF). And elemental distributions were embodied by using the energy dispersive spectroscopy (EDS) (Super-X, Bruker, Germany) and electron energy loss spectroscopy (EELS) (Quantum, Gatan, USA). The combination of a spherical aberration corrector of the gun lens allowed 0.078 nm special resolution in HAADF mode and 1.7-1.8 eV energy resolution at 200 kV. For HAADF imaging pictures, observe multiple areas of each sample to ensure that the image represents the overall situation. The electron probe was scanned over a selected area and collected at

0 to 40 keV at 5 eV/channel. Each Fe oxide phase is identified according to its morphology, in which the Sch mineral aggregates usually have a cloud-like loose porous structure, the goethite nanoparticles have a needle-like rod shape, and the humboldtine particles have a rectangular shape. The EDS line scans were used to characterize the Fe, O, S and Cr distributions, and EELS line scans were used to characterize microanalytical C distributions. The diameter of condenser lens holder was selected at 70 μm. The state of EELS line scans is energy 230.0 eV and each step is 5.00 Å. In order to obtain representative mineral micromorphological characteristics, 9-12 different regions were examined for each sample during the HADDF-STEM test.
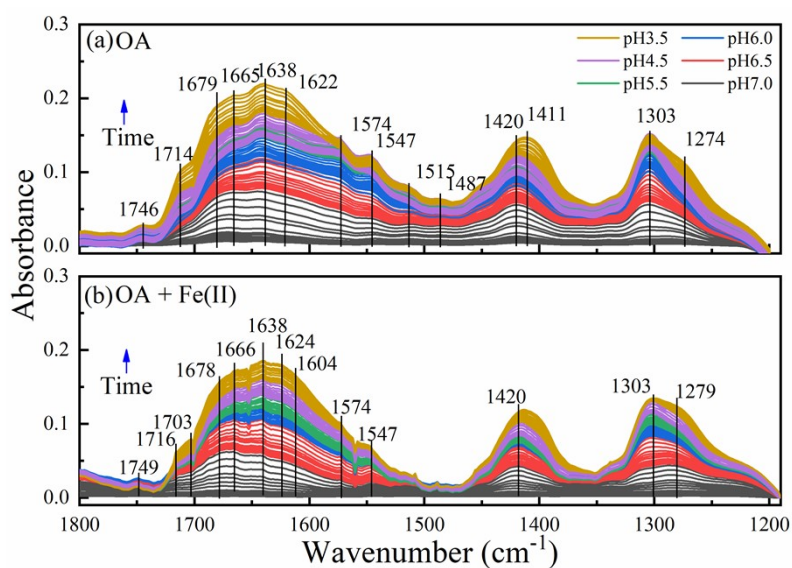
Fig S1. ATR-FTIR data of adsorbed (a) OA and (b) OA + Fe(II) during adsorption at different pH (3.5, 4.5, 5.5, 6.0, 6.5 and 7.0), [OA] = 100 μM, OA : Fe(II) = 1:1. The representative ATR-FTIR spectra of each pH were collected as a function of time ranged between 0 and 360 min.
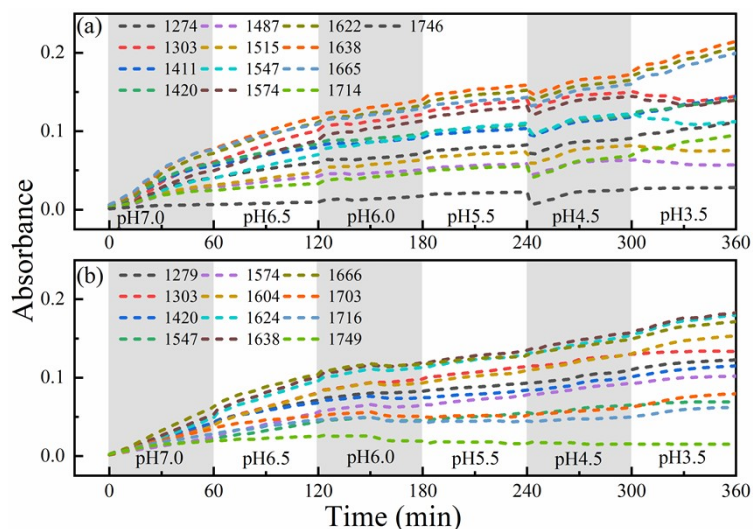
Fig. S2. Kinetic curves of the (a) OA and (b) OA + Fe(II) adsorption on Sch followed at typical peak positions under different pH. The representative ATR-FTIR spectra of each pH were collected as a function of time ranged between 0 and 360 min.
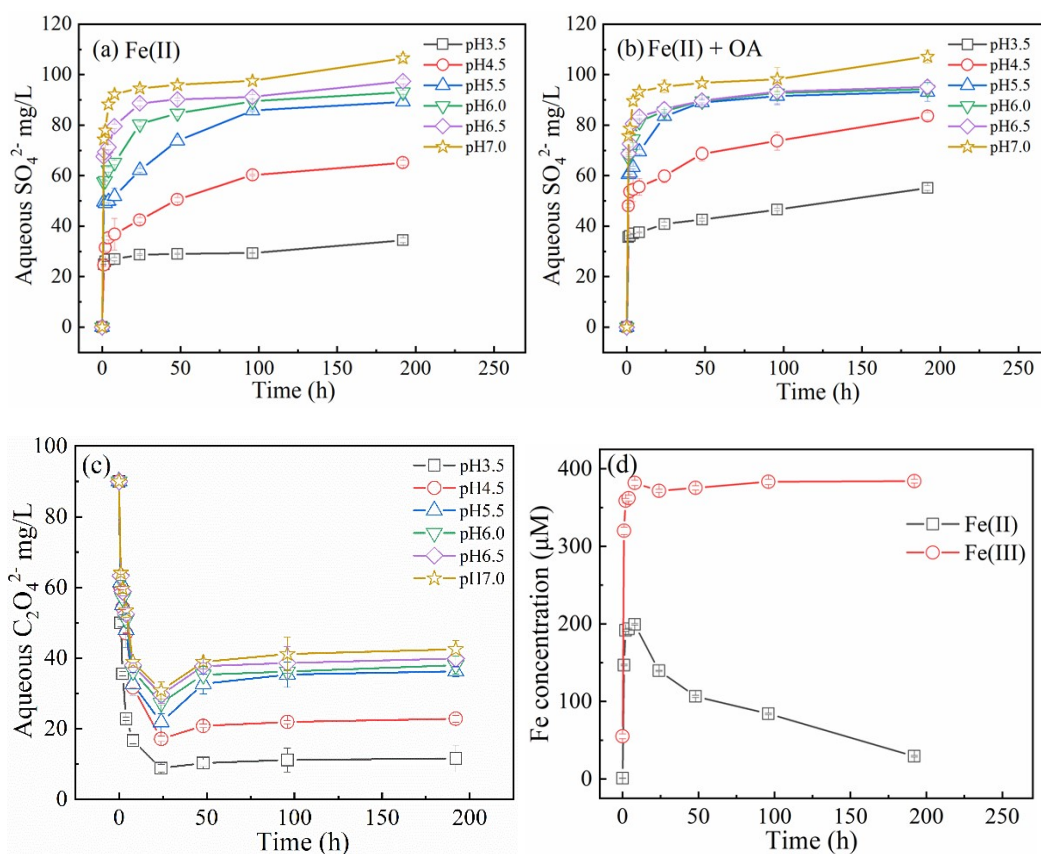
Fig. S3. Variation curves of dissolved SO_4^{2-} (a, b) and $C_2O_4^{2-}$ (c) during the experiment over 8 d. (d)Variation curves of dissolved Fe(II)/Fe(III) during the experiment over 8 d in only OA treatments at pH 3.5. Error bars are ± standard deviation of triplicates.
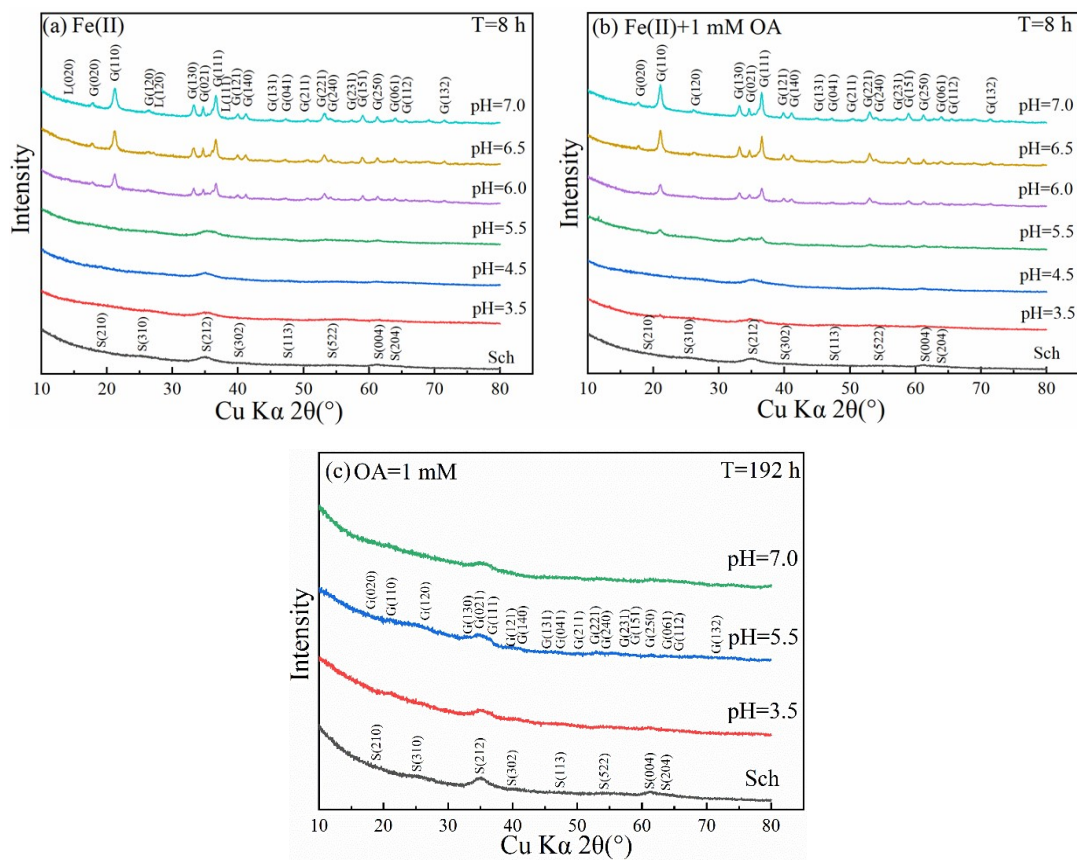
Fig. S4. X-ray diffraction (XRD) patterns of products in different treatments over 8 h. (a) with 1-mM Fe(II); (b) 1-mM Fe(II) + 1-mM oxalic acid; (c) 1-mM oxalic acid over 192 h.
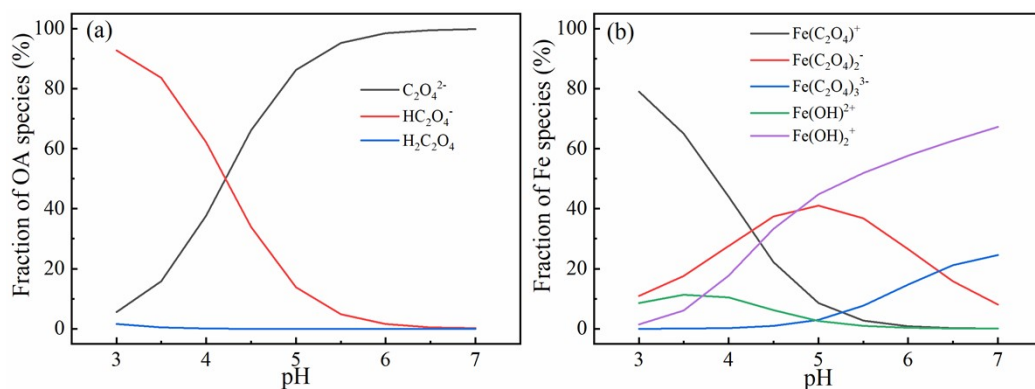
Fig. S5. The distribution of different oxalic acid and Fe(III)-oxalate complexes species with the increasing of solution pH. The reaction condition is 1 mM oxalic acid, and 1 mM Fe(III) + 1 mM oxalic acid. For the selection of ion concentration, the experimental conditions and charge balance were considered under Fe(III)-OA species fraction calculation process. The data of species were calculated by Visual MINTEQ 3.1.
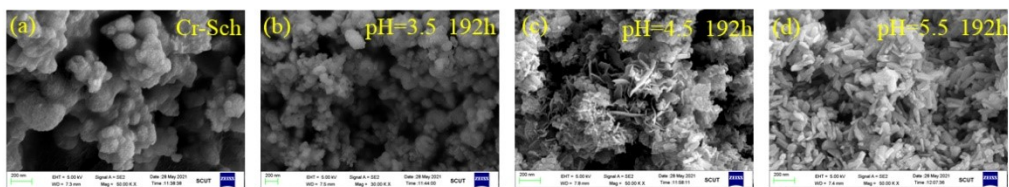
Fig. S6. Scanning Electron Microscope (SEM) graphs of samples prior to and after reaction 192 h in treatment with 1-mM Fe(II) (a-d).
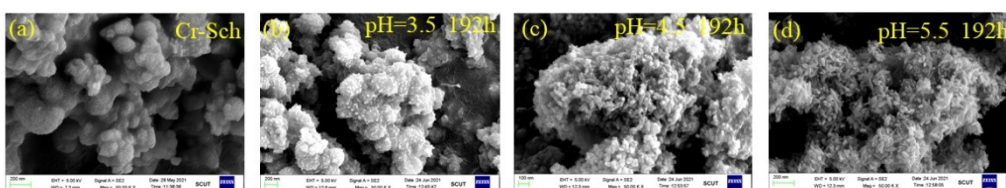
Fig. S7. SEM graphs of samples prior to and after reaction 192 h in treatment with 1-mM Fe(II) + 1-mM OA (a-d).
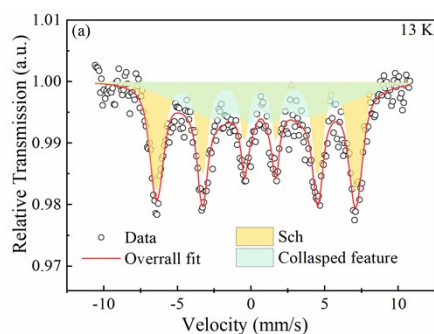
Fig. S8. Mössbauer spectra obtained at 13 K for samples in treatments with (a) original schwertmannite.
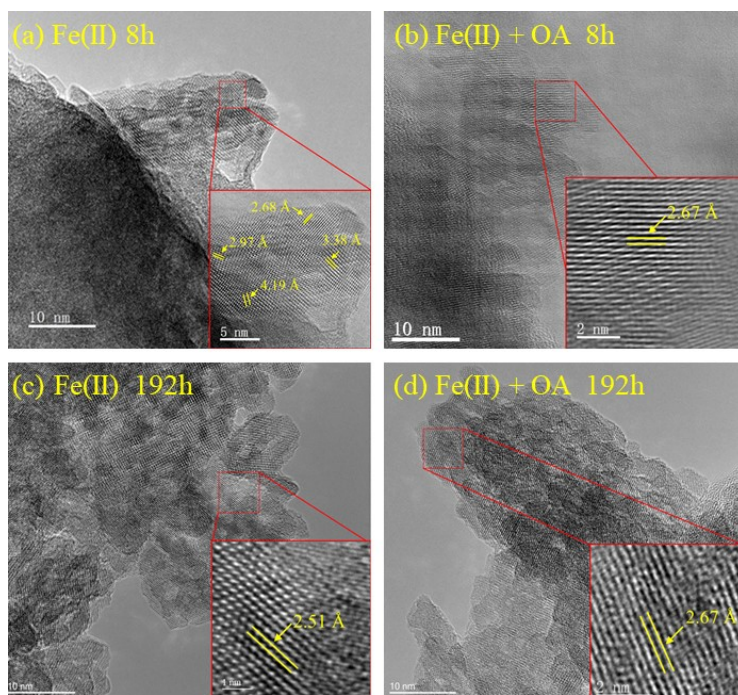
Fig. S9. TEM images of samples at 8 h Fe(II) treatment (a) and Fe(II) + OA treatment (b); 192 h Fe(II) treatment (c) and Fe(II) + OA (d) treatment.
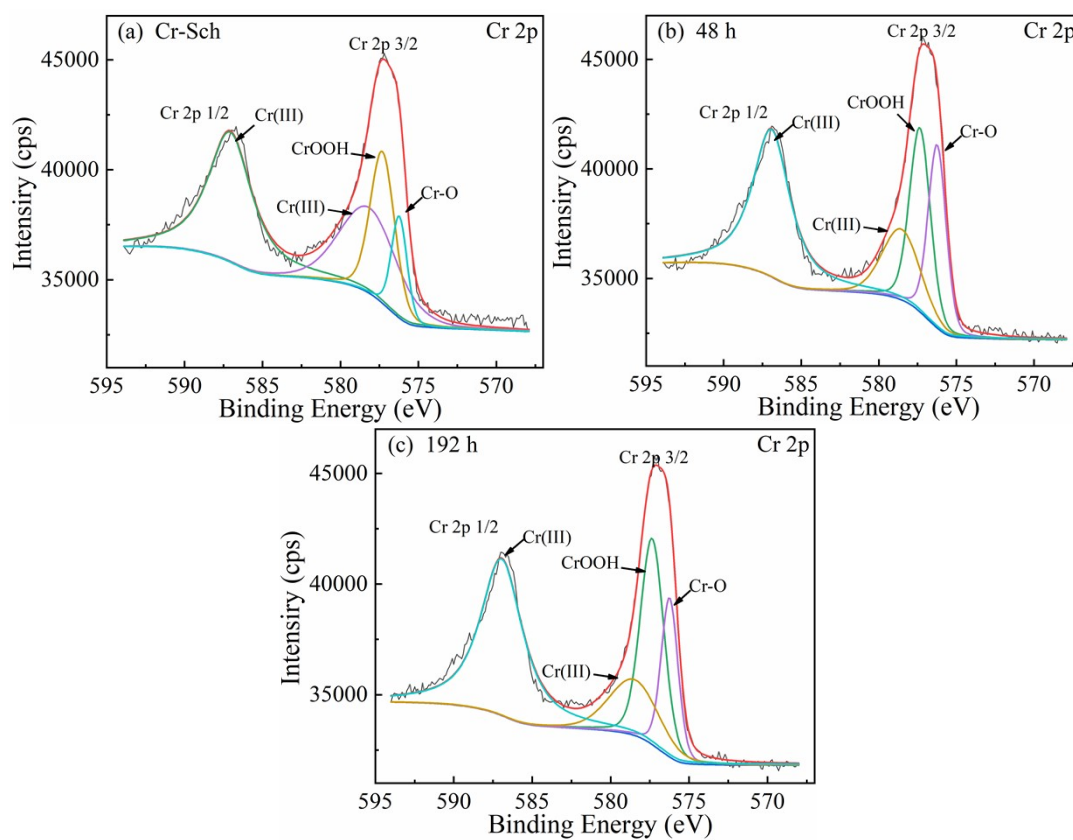
Fig. S10. XPS spectra of the solid samples taken at different times in 1 mM Fe(III) + 1 mM OA. (a) represented for Cr2p at 0 h; (b-c) represented for Cr2p at 48 and 192 h.
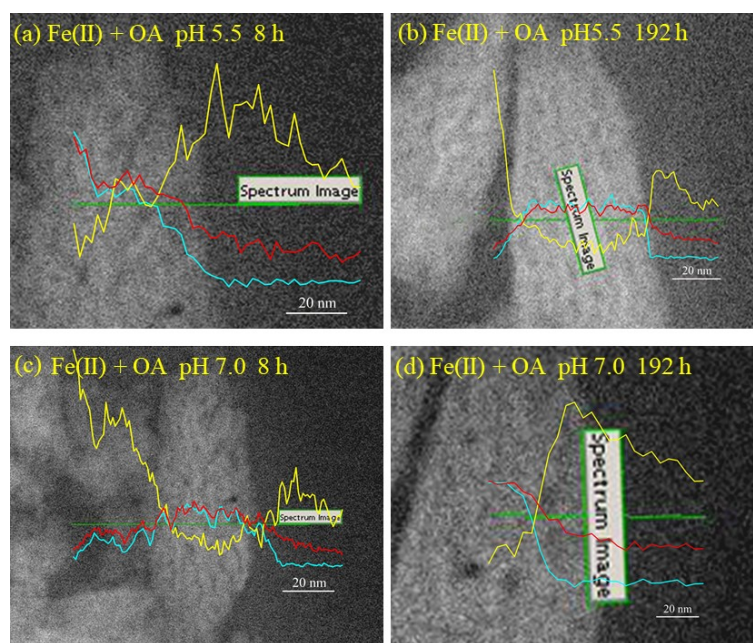
Fig. S11. EELS results of C (yellow) distribution on Fe mineral particles at 192 h Fe(II) treatment (a) and Fe(II) + OA treatment (b); 192 h Fe(II) treatment (c) and Fe(II) + OA (d) treatment. Fe (cyan), O (red).

Table S1

Mössbauer parameters used in fitting models for ~13 K Spectra.

Treatment systems	Mineral phase	δ (mm/s)	ΔE_Q (mm/s)	B_{hf} (kOe)	Lorentzian HWHM (mm/s)	Area (%)
Original mineral	Cr(III)-Sch	0.477	-0.135	419.523	0.284	100
8 h-Fe(II)	Lep	0.459	0.058	441.537	0.266	24
	Goe	0.504	-0.144	479.175	0.266	76
8h-Fe(II)-OA	Goe	0.479	-0.110	476.988	0.349	100
192 h-Fe(II)	Goe	0.475	-0.125	487.572	0.314	100
192 h-Fe(II)-OA	Goe	0.483	-0.124	488.451	0.231	100

δ: Isomer or center shift.
ΔE_Q: Quadrupole splitting.
B_{hf}: Internal magnetic field.
Lorentzian HWHM: Half width half maximum of Lorentzian lineshape (global parameter).
Area: Subspectral area ratio.

Reference

1. G. Choppala and E. D. Burton, Chromium(III) substitution inhibits the Fe(II)-accelerated transformation of schwertmannite, *Plos One*, 2018, **13**.

2. E. D. Burton, R. T. Bush and L. A. Sullivan, Sedimentary iron geochemistry in acidic waterways associated with coastal lowland acid sulfate soils, *Geochimica Et Cosmochimica Acta*, 2006,

70, 5455-5468.

3.   K. H. Knorr and C. Blodau, Experimentally altered groundwater inflow remobilizes acidity from sediments of an iron rich and acidic lake, *Environmental Science & Technology*, 2006, **40**, 2944-2950.

4.   W. Yan, J. Zhang and C. Jing, Adsorption of Enrofloxacin on montmorillonite: Two-dimensional correlation ATR/FTIR spectroscopy study, *Journal of Colloid and Interface Science*, 2013, **390**, 196-203.

5.   I. Noda, Two-dimensional correlation spectroscopy — Biannual survey 2007–2009, *Journal of Molecular Structure*, 2010, **974**, 3-24.

6.   D. G. Rancourt and J. Y. Ping, Voigt-based methods for arbitrary-shape static hyperfine parameter distributions in Mössbauer spectroscopy, *Nuclear Instruments and Methods in Physics Research Section B: Beam Interactions with Materials and Atoms*, 1991, **58**, 85-97.